A Study of Reduction and Adsorption on $LaRhO_3$

J. M. D. Tascon,† A. M. O. Olivan,‡ L. Gonzalez Tejuca,*† and Alexis T. Bell§

Instituto de Catalisis y Petroleoquimica, C.S.I.C., Serrano 119, 28006 Madrid, Spain, Departamento de Quimica General, Facultad de Ciencias, Universidad de Santander, Santander, Spain, and Department of Chemical Engineering, University of California, Berkeley, California 94720 *(Received: July 8, 1985)*

The reduction of $LaRhO_3$ and also the adsorption of H_2, CO, and NO on this perovskite have been studied. Reduction starts at 475 K and occurs in a single step with formation of La_2O_3, metallic Rh, and small amounts of Rh_2O_3. By reduction and reoxidation of $LaRhO_3$ at 1173 K a perovskite of particle size lower than that of the starting sample (preparation temperature, 973 K) was obtained. The kinetic data suggest that the reduction process occurs according to the contracting sphere model. An activation energy of reduction of 128 kJ mol^{-1} was calculated. Coverages (θ) of H_2 and CO adsorbed on $LaRhO_3$ at room temperature were lower than 1%. Coadsorption data suggest that the irreversible parts of H_2 and CO adsorb on different centers (noncompetitive adsorption). However, the reversible parts of H_2 and CO seem to compete with the irreversible parts of CO and H_2, respectively, for the same adsorption centers. Coverages of NO on $LaRhO_3$ at temperatures of 195–423 K were lower than 25%. Above 590 K θ increased considerably. NO adsorption between 140 and 340 K and at 50 mmHg appears to be fairly constant. A 1:1 correspondence between surface Rh^{3+} ions and molecules of adsorbed NO per surface unit was not found. A method for oxides characterization based on NO adsorption is suggested.

Introduction

The conversion of synthesis gas (a mixture of CO and H_2) to oxygenated organic compounds (mainly alcohols) is a subject of considerable interest as methanol and higher alcohols can be converted readily to gasoline. Exploratory research conducted during the past few years has shown that catalysts selective for this kind of reactions can be obtained by combining a noble metal (Pd, Pt, Rh) with a rare earth oxide (La_2O_3, Nd_2O_3, CeO_2). For example, Bell et al.[1-3] observed high catalytic activities in Pd supported on La_2O_3. These activities were found to be remarkably higher than that of Pd supported on SiO_2. Similar effects were oberved by Kuznetsov et al.[4] for Rh supported on SiO_2, Al_2O_3, and La_2O_3.

A different way to combine a noble metal with a rare earth oxide would be through perovskite-type compounds ($LaRhO_3$, $CePdO_3$). Watson and Somorjai[5] associated the ability of $LaRhO_3$ to yield oxygenated compounds to an oxidation state of Rh higher than zero. In this catalyst metallic Rh is, probably, responsible for the dissociative adsorption of CO and chain growth with formation of alkanes and alkenes while oxidized species of Rh induce carbonylation with formation of oxygenated products. In fact, those authors found on the surface of this perovskite in reaction conditions metallic Rh and Rh^{1+}. In this work the changes in $LaRhO_3$ with temperature in the presence of H_2 have been studied by means of temperature-programmed reduction, kinetics of reduction, and X-ray diffraction. Experiments of successive adsorption of H_2 and CO on this oxide were, also, carried out. This information should be useful for reactions of H_2 + CO which are catalyzed by this or similar perovskites having in positions A and B of the structure a rare-earth metal and a noble metal, respectively. Finally, experiments of NO adsorption to test the usefulness of this molecule for the characterization of active centers in position B were performed. In a second stage it is intended to investigate the influence of the oxidation state of the noble metal in the catalytic activity of these compounds.

Experimental Section

Materials. $LaRhO_3$ was prepared by precipitating the metallic ions from an equimolar solution of $La(NO_3)_3 \cdot 6H_2O$ (Merck, p.a.) and $RhCl_3 \cdot xH_2O$ (Fluka AG, puriss.; by means of thermogravimetric analysis a value of x = 3.4 was determined) with tetraethylammonium hydroxide $(C_2H_5)_4NOH$ using twice the stoichiometrically required amount, according to a method previously described.[6] The precipitate was dried at 373 K and then heated at 973 K in air for 24 h. The resulting black powder had a BET specific surface area (0.162 nm^2 for the cross-sectional area of N_2) of 4.24 m^2 g^{-1}. In the X-ray diffractogram (Figure 2d) only characteristic peaks of the perovskite were found. CO 99.97% pure was condensed at 77 K and distilled taking for storage the middle fraction. H_2 and He, both 99.995% pure, were passed through a trap at 77 K.

Equipment and Methods. Temperature-programmed reduction (TPR) and reduction kinetics experiments were carried out with a Cahn 2100 RG microbalance connected to a high-vacuum system in which a dynamic vacuum of 10^{-6} mmHg (1 mmHg = 133.3 nm^{-2}) could be maintained. The gravimetric measurements had an accuracy of 10^{-5} g. For TPR a sample of ca. 70 mg of powder was laid into the microbalance cylindrical weighing pan (1 cm diameter, 0.5 cm high) and then it was pumped at room temperature (rt) for 1 h and contacted with 200 mmHg of H_2 (static conditions). After this the temperature was raised at a rate of 4 K min^{-1} by means of a Stanton Redcroft Eurotherm temperature programmer. The weight loss was taken as a measure of the reduction degree. For kinetics of reduction, the sample (as above) was pumped at rt for 1 h, heated at the desired temperature, and then contacted with 200 mmHg of H_2 (static conditions); weight changes were recorded for 40–70 min. For each isothermal run a fresh sample was taken. X-ray diffractograms of samples after reduction in H_2 (200 mmHg, 1 h) and after sintering in He (200 mmHg, 1 h) or reoxidation in air (700 mmHg, 1 h) were obtained with a Philips PW/1010 diffractometer using Cu Kα radiation and a Ni filter. Some samples used in TPR (Figure 1) or in isothermal runs (Figure 3) were also taken for X-ray diffraction. They will be denoted by (TPR) or (isotherm). Their reduction degree can, therefore, be found in their respective TPR diagram or kinetic curve.

Adsorption experiments were carried out in a standard volumetric apparatus. Pressure measurements were made with an MKS 310 BHS-1000 transducer with an accuracy of 10^{-2} mmHg. The sample (ca. 500 mg of powder) was first outgassed at 773 K for 15 h in high vacuum and then cooled to rt. After this, successive doses of H_2 were admitted into the adsorption cell (ca. 10 cm^3) (total adsorption of H_2 on a clean surface). After pumping (rt, 1 h) a second isotherm was carried out (reversible adsorption

† Instituto de Catalisis y Petroleoquimica.
‡ Universidad de Santander.
§ University of California.

(1) Hicks, R. F.; Yen, Q.-J.; Bell, A. T. *J. Catal.* **1984**, *89*, 498.
(2) Hicks, R. F.; Bell, A. T. *J. Catal.* **1984**, *90*, 205.
(3) Hicks, R. F; Bell, A. T. *J. Catal.* **1985**, *91*, 104.
(4) Kuznetsov, V. L.; Romanenko, A. V.; Mudrakovskii, I. L.; Mastikhin, V. M.; Shmachkov, V. A.; Yermakov, Yu. I. "Proceedings of the 8th International Congress on Catalysis", Verlag Chemie: Weinheim, West Germany, 1984; Vol. V, p 3.
(5) Watson, P. R.; Somorjai, G. A. *J. Catal.* **1982**, *74*, 282.
(6) Crespin, M.; Hall, W. K. *J. Catal.* **1981**, *69*, 359.

0022-3654/86/2090-0791$01.50/0

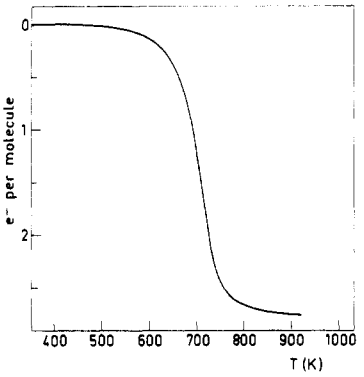

Figure 1. Temperature-programmed reduction (4 K min^{-1}) of $LaRhO_3$ in 200 mmHg of H_2.

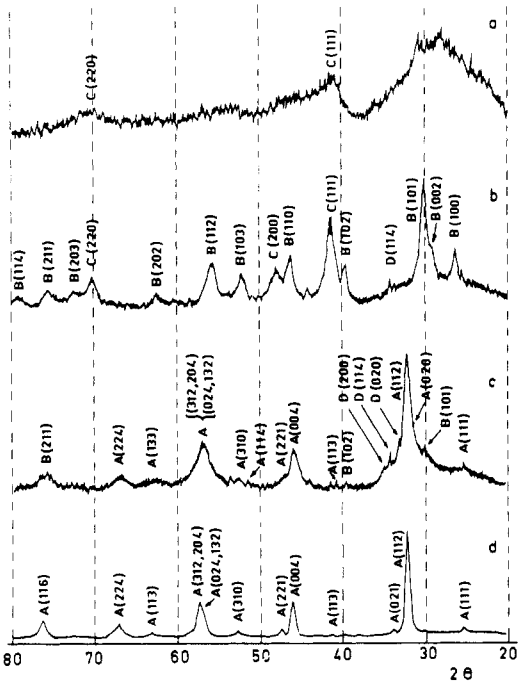

Figure 2. X-ray diffraction patterns (Cu Kα radiation) of $LaRhO_3$ after treatments of reduction in H_2, reoxidation in air, and/or sintering in He: (a) reduction at 773 K; (b) reduction at 773 K and sintering at 1173 K; (c) reduction at 973 K and reoxidation and 973 K; and (d) reduction at 1173 K and reoxidation at 1173 K. A, $LaRhO_3$; B, La_2O_3; C, Rh; D, Rh_2O_3. For additional description of treatments see text.

of H_2). The sample was then pumped (rt, 1 h) and dosed with CO (total adsorption of CO on a surface with preadsorbed H_2). Finally, after pumping (rt, 1 h) a second isotherm was run (reversible adsorption of CO). After outgassing at 773 K for 15 h similar experiments adsorbing CO first and then H_2 were carried out. As for H_2 or CO, the sample was outgassed at 773 K for 15 h before an experiment of NO adsorption.

Results and Discussion

Temperature-Programmed Reduction. TPR data (H_2) in terms of electrons (e^-) per molecule (3 e^- per molecule amount of full reduction of Rh^{3+} to metallic Rh) vs. temperature are plotted in Figure 1. At 4 K min^{-1} reduction starts at about 475 K, the maximum slope of the curve (weight loss per degree centrigrade) being recorded at ca. 700 K. Above 775 K the slope decreases rapidly and at 1000 K a plateau corresponding to a reduction of 2.75 e^- per molecule is reached. Reduction in H_2 of oxidized rhodium supported on SiO_2, Al_2O_3, La_2O_3, and TiO_2[7-9] started

TABLE I: Particle Sizes of $LaRhO_3$ Determined by X-ray Line Broadening

treatment of the starting sample[a]	B, deg	β, rad	d, Å
starting sample	0.46	0.0075	192
reduction at 973 K and reoxidation at 973 K	0.88	0.0151	95
reduction at 1173 K and reoxidation at 1173 K	0.51	0.0084	171

[a] For description of treatments see text.

TABLE II: Particle Sizes of La_2O_3 (B) and Rh (C) Determined by X-ray Line Broadening

treatment of the starting sample[a]	B, deg	β, rad	d, Å
reduction at 673–773 K			25–40 (C)
reduction at 973 K	0.88	0.0151	95 (B)
	1.73	0.0301	49 (C)
reduction at 1173 K	0.85	0.0146	98 (B)
	1.35	0.0234	63 (C)
reduction at 773 K and	0.71	0.0121	119 (B)
sintering at 1173 K	1.18	0.0204	73 (C)

[a] For description of treatments see text.

and exhibited rate maxima of weight loss at lower temperatures than those in Figure 1, indicating a higher stability of Rh^{3+} in the perovskite structure. Unlike other perovskites of group VIII (groups 8–10)[53] metals, e.g., $LaCoO_3$[6,10] and $LaNiO_3$,[11,12] no stable intermediate reduction states have been detected; i.e., rhodium presented no stable oxidation states between 3+ and 0. Rh(I) has been found, however, in the reduction (by heating in vacuum) of Rh–Y zeolites,[13,14] $LaRhO_3$ underwent nearly full reduction at temperatures slightly higher than those where $LaCoO_3$[6] and $LaNiO_3$[12] reduced to 3 e^- per molecule. $LaMnO_3$ and $LaFeO_3$[15] reduced at higher temperatures.

X-ray Diffraction. X-ray patterns after treatments of reduction in H_2, reoxidation in air and/or sintering in He of $LaRhO_3$ are given in Figure 2. After reduction at 673 or 773 K (isotherm) the perovskite structure is destroyed (pattern 2a). The reduced material is rather amorphous and only peaks of metallic Rh and not well-defined peaks of La_2O_3 (between 28 and 31°) were present. However, after reduction at 773 K and sintering at 1173 K well-defined peaks of La_2O_3, Rh, and Rh_2O_3 were observed (pattern 2b). $LaRhO_3$ reduced at 973 K yielded a pattern similar to that in 2b. After this treatment and reoxidation at 973 K (pattern 3c) Rh is oxidized to Rh_2O_3 which reacts with La_2O_3 producing $LaRhO_3$. Notwithstanding, the conversion of simple oxides to perovskite is incomplete. Even after reduction at 1173 K (TPR) (pattern not shown) the most intense peak of Rh_2O_3 (114) was detected. This unreduced rhodium may account for the incomplete reduction observed in the TPR in Figure 1. After reduction at 1173 K (TPR) and reoxidation at the same temperature (pattern 2d) only peaks of the perovskite structure were observed.

These results together with the TPR data indicate that the reduction of $LaRhO_3$ occurs in a single step with formation of La_2O_3, metallic Rh, and small amounts of unreduced Rh_2O_3 according to the reaction,

$$2LaRhO_3 + 3xH_2 \rightarrow La_2O_3 + 2xRh + (1 - x)Rh_2O_3 + 3xH_2O \quad (1)$$

(7) Yao, H. C.; Japar, S.; Shelef, M. *J. Catal.* **1977**, *50*, 407.
(8) Kuznetsov, V. L.; Mudrakovskii, I. L.; Romanenko, A. V.; Pashis, A. V.; Mastikhin, V. M.; Yermakov, Yu. I. *React. Kinet. Catal. Lett.* **1984**, *25*, 137.
(9) Vis, J. C.; Van't Blik, H. F. J.; Huizinga, T.; Van Grondelle, J.; Prins, R. *J. Mol. Catal.* **1984**, *25*, 367.
(10) Nakamura, T.; Petzow, G.; Gauckler, L. J. *Mater. Res. Bull.* **1979**, *14*, 649.
(11) Crespin, M.; Levitz, P.; Gatineau, L. *J. Chem. Soc., Faraday Trans. 2* **1983**, *79*, 1181.
(12) Fierro, J. L. G.; Tascón, J. M. D.; González Tejuca, L. *J. Catal.* **1985**, *93*, 83.
(13) Okamato, Y.; Ishida, N.; Imanaka, T.; Teranishi, S. *J. Catal.* **1979**, *58*, 82.
(14) Iizuka, T.; Lunsford, J. H. *J. Mol. Catal.* **1980**, *8*, 391.
(15) Fierro, J. L. G.; Tascón, J. M. D.; González Tejuca, L. *J. Catal.* **1984**, *89*, 209. Tascón, J. M. D.; Fierro, J. L. G.; González Tejuca, L. *J. Chem. Soc., Faraday Trans. 1*, **1985**, *81*, 2399.

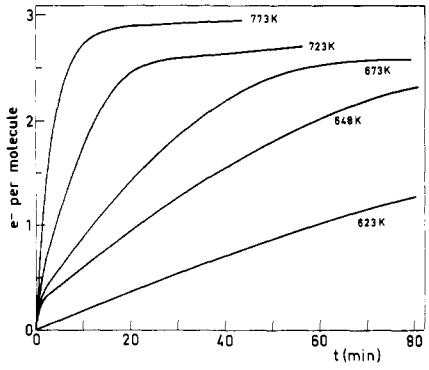

Figure 3. Kinetics of reduction of $LaRhO_3$ in 200 mmHg of H_2.

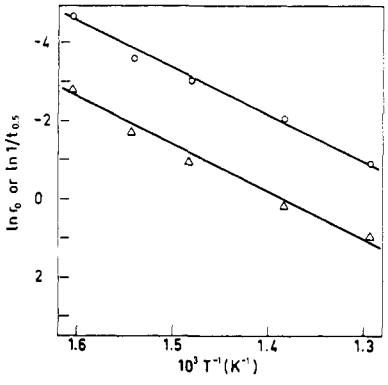

Figure 4. Plots of ln $1/t_{0.5}$ (O) ($t_{0.5}$, time needed for reduction to 1.5 e^- per molecule) and ln r_0 (Δ) (r_0, initial reduction rate) vs. $1/T$.

By means of the Debye–Scherrer equation[16] $d = K\lambda/\beta \cos\theta$ (K, constant which was taken as 0.9; λ, wavelength of the X-ray used; β, broadening of the line chosen as given by $\beta = (B^2 - b^2)^{1/2}$, B being the experimental width and b the reference width measurement under the same experimental conditions with a sample of particle size higher than 1000 Å, 1 Å = 10^{-1} nm; θ, diffraction angle of the line considered), particle sizes of the initial $LaRhO_3$ as well as sizes of the resulting perovskite, La_2O_3, and Rh after different treatments were calculated. For this, the most intense peaks of the metal (111) and of oxides ((112) for $LaRhO_3$, (101) for La_2O_3)) were taken. The values obtained are given in Tables I and II. After reduction and reoxidation at 973 K (temperature used in the final heating during preparation of $LaRhO_3$), a perovskite of particle size substantially lower (95 Å, Table I) than that of the starting sample (192 Å) was obtained. Similar effects were observed by Reller et al.[17] in $CaRuO_3$ single crystals. The particle diameter, d, increased with increasing treatment temperature although after reduction (TPR) and reoxidation at 1173 K, it was found to be smaller (171 Å) than the starting particle size of the perovskite. After reduction of $LaRhO_3$ at 673–773 K (isotherm) highly dispersed Rh (d = 25–40 Å) was obtained (Table II). The particle sizes of both Rh and La_2O_3 increased remarkably with increasing reduction temperature. After treatments of $LaRhO_3$ in H_2 at 773 K and He at 1173 K they were higher than those obtained after heating the perovskite in H_2 at 1173 K (TPR); i.e., sintering in He seems to be faster than sintering in a reducing atmosphere.

Kinetics of Reduction. The kinetics of $LaRhO_3$ reduction by H_2 in the temperature interval 623–773 K are plotted in Figure 3. The reduction rate decreases continually with time. This behavior is consistent with the contracting sphere model[18] according to which the oxide grains are covered in the first reduction stages by a layer of metallic rhodium. In this case the rate of the interfacial reaction decreases with time as the grains of $LaRhO_3$ are consumed in the reaction.

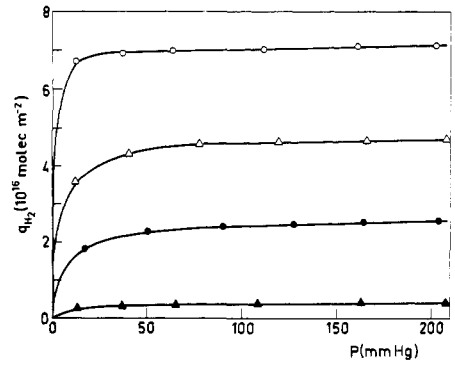

Figure 5. Total (empty symbols) and reversible (solid symbols) adsorption of H_2 on a clean surface of $LaRhO_3$ at room temperature (circles) and on a surface with preadsorbed CO (triangles).

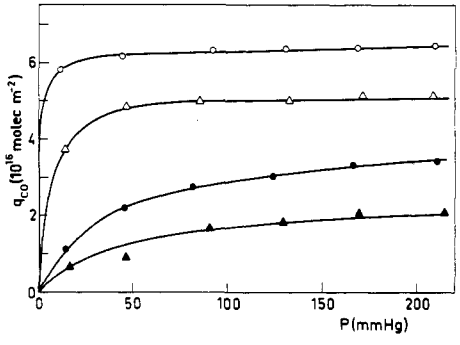

Figure 6. Total (empty symbols) and reversible (solid symbols) adsorption of CO on a clean surface of $LaRhO_3$ at room temperature (circles) and on a surface with preadsorbed H_2 (triangles).

The activation energy of reduction (E_a) was calculated from Arrhenius plots of ln r_0 (r_0, initial reduction rate determined analytically by fitting the kinetic data to a polynomic function and differentiation to time zero) vs. $1/T$ and ln $1/t_{0.5}$ ($t_{0.5}$, time needed for a reducing half of that of the total reduction process) vs. $1/T$ (Figure 4). E_a values were, respectively, 138 and 118 kJ mol^{-1}. The mean E_a, 128 kJ mol^{-1}, is remarkably loweer than those found for reduction to 3 e^- per molecule of other perovskites of group VIII metals (for $LaNiO_3$ and $LaFeO_3$, $E_a \simeq 200$ kJ mol^{-1}).[12,15] The fair agreement among E_a values calculated by the different methods shows the internal consistency of the data.

Adsorption of H_2 and CO and Coadsorption H_2–CO. Surface interactions of H_2 and CO have been observed on Rh supported on La_2O_3 at ca. 353 K.[19] These may give place to a surface compound and to enhanced adsorption of H_2 and CO after preadsorption of the other molecule.[20,21] Therefore, these adsorption experiments were carried out at room temperature. The isotherms obtained are given in Figures 5 and 6. The adsorption of H_2 and CO at 200 mmHg on a clean surfce ((6–7) × 10^{16} molecules m^{-2}) is remarkably lower than the adsorption of CO on $LaMO_3$ oxides (M, first-row transition metal, from Cr to Ni),[22] and SnO_2,[23] and, also, lower than the adsorption of H_2 and CO on supported group VIII metals (Pd·La_2O_3, Ru powder, and Ni·SiO_2).[1,24–26] On the other hand, the ratio CO/H is lower than

(16) Jelinek, Z. K. "Particle Size Analysis"; Ellis Horwood: New York, 1974; Series in Analytical Chemistry, Chapter 2.
(17) Reller, A.; Davoodabady, G.; Portmann, A.; Oswald, H. R. "Proceedings of the 8th European Congress on Electron Microscopy"; Csanády, A., Röhlich, P., Szabó, D., Eds.; Programme Committee of the 8th European Congress on Electron Microscopy: Budapest, Hungary, 1984; Vol. 2, p 1165.
(18) Hurst, N. W.; Gentry, S. J.; Jones, A. *Catal. Rev.-Sci. Eng.* **1982**, *24*, 233.
(19) Kuznetsov, V. L.; Mudrakowskii, I. L.; Romanenko, A. V.; Mastikhin, V. M.; Yermakov, Yu. I. *React. Kinet. Catal. Lett.* **1984**, *25*, 147.
(20) Gupta, R. B.; Viswanathan, B.; Sastri, M. V. C. *J. Catal.* **1972**, *26*, 212.
(21) Kung, H. H. *Catal. Rev.-Sci. Eng.* **1980**, *22*, 235.
(22) Tascón, J. M. D.; González Tejuca, L.; Rochester, C. H. *J. Catal.* **1985**, *95*, 558.
(23) Solymosi, F.; Kiss, J. *J. Catal.* **1978**, *54*, 42.
(24) McKee, D. W. *J. Catal.* **1967**, *8*, 249.
(25) Winslow, P.; Bell, A. T. *J. Catal.* **1985**, *91*, 142.
(26) Prinsloo, J. J.; Gravelle, P. C. *J. Chem. Soc., Faraday Trans. 1* **1980**, *76*, 512.

TABLE III: Coverages of H_2 and CO (θ_{H_2}, θ_{CO}) at 200 mmHg on $LaRhO_3$ at 298 K

surface	adsorption	θ_{H_2}[a]	θ_{CO}[b]
clean	irreversible	0.56×10^{-2}	0.45×10^{-2}
clean	reversible	0.31×10^{-2}	0.52×10^{-2}
preadsorbed CO (or H_2)	irreversible	0.53×10^{-2}	0.46×10^{-2}
preadsorbed CO (or H_2)	reversible	0.05×10^{-2}	0.31×10^{-2}

[a] Cross-sectional area of H_2, 12.3 Å^2. [b] Cross-sectional area of CO, 15.1 Å^2.

unity, in agreement with what has been observed for supported Ni[26] and Rh[27] catalysts.

Coverages for total adsorption (taking as cross-sectional areas of H_2 and CO, 12.3 and 15.1 Å^2, respectively[28]) (Table III) are lower than 1%. The fractions of irreversibly adsorbed H_2 or CO are not affected by preadsorption of the other molecule. This suggests that these parts adsorb on centers of a different nature. Probably, CO adsorbs on surface oxide ions yielding carbonates, as shown for other $LaMO_3$ oxides,[29] while H_2 adsorbs on transition-metal ions (Rh^{3+}). However, the reversibly adsorbed parts of H_2 and CO decreased considerably after preadsorption of CO or H_2 and is much more marked for CO preadsorption. No steric hindrance should be involved here because of the low coverages reached. Rather, these results may be indicative of the reversible adsorption of H_2 and CO which compete for the same adsorption centers involved in the adsorption of the irreversibly adsorbed parts of CO and H_2, respectively; i.e., reversible CO would adsorb on Rh^{3+} while reversible H_2 would adsorb on oxide ions yielding OH^-. Formation of carbonates as well as linear and bridged CO after adsorption of H_2 + CO on supported rhodium was reported by Solymosi et al.[30] In any case, the dependence of the reversible adsorption of both molecules on the state of the adsorbent surface (clean or with preadsorbed CO or H_2) points to a chemisorption character of these fractions. Competitive adsorption of H_2 and CO has also been observed by Hecker and Bell on Rh·SiO_2,[31] by Prinsloo and Gravelle on Ni·SiO_2,[26] and by Gopalakrishnan and Viswanathan on unsupported cobalt.[32] Solymosi et al.[30] found that the adsorption of H_2 on supported rhodium does not influence in any noticeable extent the adsorption of CO. Enhanced adsorption of H_2 and/or CO after preadsorption of CO of H_2 has been reported on ruthenium powder,[24] on cobalt–thoria–kieselguhr,[20,33] and on zinc[21] catalysts.

No Adsorption and Metallic Centers. Isotherms of NO adsorption on $LaRhO_3$ in the temperature zone 195–773 K are given in Figure 7. Coverages (θ) at 150 mmHg (taking as cross-sectional area of NO 15.38 Å^2/molecule which is the mean value of the cross-sectional areas calculated from the adsorption at $\theta = 1$ given by Shelef et al. for Cr_2O_3, MnO, Fe_2O_3, Co_3O_4, NiO, and CuO[34–39] between 195 and 423 K) are lower than 25%. However, at 591 and 773 K θ increases considerably reaching one monolayer at this last temperature. These coverages are of the same order as those found on $LaMO_3$ oxides[22] and also on simple oxides.[34–39] The isobars for adsorption are given in Figure 8. The increase of q_{NO} with temperature is pronounced at 150 mmHg and less marked at 50 mmHg. At this last pressure q_{NO} appears to be fairly constant between 140 and 340 K; on other perovskites q_{NO} was found to be constant in a wider range of temperatures

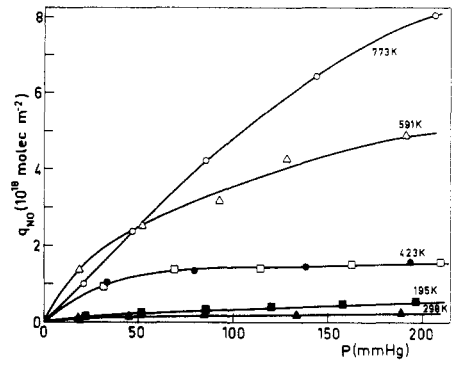

Figure 7. Isotherms of NO adsorption on $LaRhO_3$: □, ●, duplicated run.

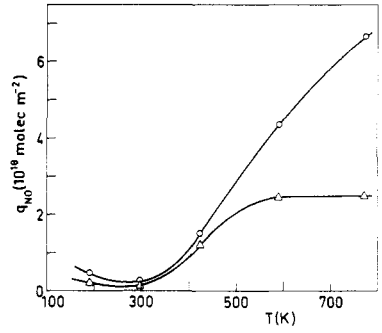

Figure 8. Isobars of NO adsorption at 50 (△) and 150 mmHg (○) on $LaRhO_3$.

(from 200 to 600 K in NO/$LaFeO_3$;[40] from 200 to 750 K in NO/$LaNiO_3$[22]). Solymosi and Kiss observed an increase of q_{NO} with T in the system NO/SnO_2.[23,41]

The number of surface Rh^{3+} ions per m^2 in $LaRhO_3$ is 2.56 $\times 10^{18}$ considering as most exposed crystallographic planes those of lower Miller's index, (100), (110), and (111). No plateau for NO adsorption in any of the isotherms in Figure 7 equal to this number of ions or equal to its half (assuming a half-populated stable surface ayer of metal cations[42]) in $LaRhO_3$ has been found. On the other hand, the isotherms do not appear to converge to a common monolayer ($q_{NO(m)}$). On the contrary, it seems that $q_{NO(m)}$ depends strongly on the temperature. Therefore the stoichiometry $q_{NO(m)}/M_s^{n+} \simeq 1:1$ (M_s^{n+}, exposed transition-metal cations) reported by Shelef et al. for NO adsorption on simple oxides[34,36,38,39] has been observed neither in the system NO/$LaRhO_3$ nor in the systems NO/$LaMO_3$[22] previously studied in our laboratory. This should be due to the fact that NO interacts not only with transition-metal cations (yielding mononitrosyls, dinitrosyls, dimers)[43–46] but also with oxide ions yielding nitrate, nitrite, or nitro groups).[40,46,47–50]

We conclude that the NO adsorption and the application of the stoichiometry $q_{NO(m)}/M_s^{n+} \simeq 1:1$ may not give a proper estimate of the number of exposed transition-metal cations or of the fraction of surface occupied by an oxide when deposited on a support. Probably, the later quantity could be measured, though, by determining the ratio of adsorbed NO molecules per surface unit of unsupported oxide and then using this ratio for the sup-

(27) Niwa, M.; Lunsford, J. H. *J. Catal.* **1982**, *75*, 302.
(28) McClellan, A. L.; Harnsberger, H. F. *J. Colloid Interface Sci.* **1967**, *23*, 577.
(29) Tascón, J. M. D.; González Tejuca, L. *Z. Phys. Chem. (Wiesbaden)* **1980**, *121*, 63. González Tejuca, L.; Rochester, C. H.; Fierro, J. L. G.; Tascón, J. M. D. *J. Chem. Soc., Faraday Trans. 1* **1984**, *80*, 1089.
(30) Solymosi, F.; Tombacz, I.; Kocsis, M. *J. Catal.* **1982**, *75*, 78.
(31) Hecker, W. C.; Bell, A. T. *J. Catal.* **1984**, *88*, 289.
(32) Gopalakrishnan, R.; Viswanathan, B. *Surf. Technol.* **1984**, *23*, 173.
(33) Sastri, M. V. C.; Viswanathan, B. *J. Sci. Ind. Res., Sect. B* **1954**, *13*, 590.
(34) Otto, K.; Shelef, M. *J. Catal.* **1969**, *14*, 226.
(35) Yao, H. C.; Shelef, M. *J. Catal.* **1973**, *31*, 377.
(36) Otto, K.; Shelef, M. *J. Catal.* **1970**, *18*, 184.
(37) Yao, H. C.; Shelef, M. *J. Phys. Chem.* **1974**, *78*, 2490.
(38) Gandhi, H. S.; Shelef, M. *J. Catal.* **1972**, *24*, 241.
(39) Gandhi, H. S.; Shelef, M. *J. Catal.* **1973**, *28*, 1.
(40) Peña, M. A.; Tascón, J. M. D.; González Tejuca, L. *Nouv. J. Chim.* **1985**, *9*, 591.
(41) Solymosi, F.; Kiss, J. *J. Catal.* **1976**, *41*, 202.
(42) Kummer, J. T.; Yao, Y.-F. Y.; *Can. J. Chem.* **1967**, *45*, 421.
(43) Peri, J. B. *J. Phys. Chem.* **1974**, *78*, 588.
(44) Yuen, S.; Chen, Y.; Kubsh, J. E.; Dumesic, J. A.; Topsøe, N.; Topsøe, H. *J. Phys. Chem.* **1982**, *86*, 3022.
(45) Segawa, K.; Chen, Y.; Kubsh, J. E.; Delgass, W. N.; Dumesic, J. A.; Hall, W. K. *J. Catal.* **1982**, *76*, 112.
(46) King, D. L.; Peri, J. B. *J. Catal.* **1983**, *79*, 164.
(47) London, J. W.; Bell, A. T. *J. Catal.* **1973**, *31*, 32.
(48) Davydov, A. A.; Lokhov, Yu. A.; Shchekochikhin, Yu. M. *Kinet. Katal.* **1978**, *19*, 673.
(49) Rochester, C. H.; Topham, S. A. *J. Chem. Soc., Faraday Trans. 1* **1979**, *75*, 872.
(50) Busca, G.; Lorenzelli, V. *J. Catal.* **1981**, *72*, 303.

ported oxide. These measurements should be carried out in a zone where NO adsorption does not depend strongly on the temperature (for $LaRhO_3$ between 140 and 340 K and $P \leq 50$ mmHg) (Figure 8). NO has a number of advantages over other molecules such as CO and O_2 used for the characterization of oxides. CO adsorption appears to be more temperature-dependent than NO.[29] On the other hand, measurements of adsorption of individual gases and of coadsorption NO–CO seem to indicate that the adsorption bond of CO on simple[37,38,51,52] as on mixed oxides[22] is weaker than that of NO. Finally, the method of O_2 adsorption at low temperatures (77–195 K) involves the experimental determination of the irreversibly adsorbed part. This is made by the difference of the total and reversible adsorptions. Both these values are, generally, very large and this may constitute an important source of error.

Acknowledgment. We are indebted to CAICYT for sponsorship of this work. Thanks are also due to Ministerio de Educacion y Ciencia for a grant awarded to J.M.D.T. and to the Spanish-North American Joint Committee for Scientific and Technological Cooperation for financial support.

Registry No. $LaRhO_3$, 11092-15-2; CO, 630-08-0.

(51) Alexeyev, A.; Terenin, A. *J. Catal.* **1965**, *4*, 440.
(52) Raskó, J.; Solymosi, F. *Acta Chim. Acad. Sci. Hung.* **1977**, *95*, 389.

(53) In this paper the periodic group notation in parentheses is in accord with recent actions by IUPAC and ACS nomenclature committees. A and B notation is eliminated because of wide confusion. Groups IA and IIA become groups 1 and 2. The d-transition elements comprise groups 3 through 12, and the p-block elements comprise groups 13 through 18. (Note that the former Roman number designation is preserved in the last digit of the new numbering: e.g., III → 3 and 13.)

Molecular Dynamics Study of the Hydrophobic Interaction in an Aqueous Solution of Krypton

Kyoko Watanabe† and Hans C. Andersen*

Department of Chemistry, Stanford University, Stanford, California 94305 *(Received: July 19, 1985)*

We have performed molecular dynamics calculations for systems of two and several atomic solutes dissolved in a model for liquid water to study the hydrophobic association of nonpolar solutes in aqueous solution. The parameters of the potentials were chosen to be appropriate for an aqueous solution of Kr. In accordance with previous work, we find that at infinite dilution a pair of atoms has two preferred configurations, one in which they are near neighbors and another in which they are separated by a water molecule, and that the latter is more stable than the former at infinite dilution. In the simulations of systems containing several atomic solutes, the atoms were found to form clusters in which the atom–atom distances corresponded to the formation of near-neighbor and solvent-separated pairs. The number of near-neighbor pairs formed is approximately the same (within the noise of the calculation) as there would be in a random distribution of solutes in space at the same concentration, indicating that in water there is no great tendency for hydrophobic association of these solutes. The number of solvent-separated pairs is significantly less than for a random distribution of solutes. On the average, the effect of the solvent is to tend to keep the solutes apart rather than to cause them to associate. This result contradicts the conventional wisdom on hydrophobic interaction, and a new analysis of experimental solubility data gives support to the result.

I. Introduction

The phrase "hydrophobic interaction" refers to the supposed tendency for nonpolar solutes and groups dissolved in water to be associated with one another. It is usually assumed to be a major factor influencing the immiscibility of water and nonpolar substances, the thermodynamic properties of aqueous solutions, the conformations of proteins and nucleic acids in solution, association equilibria in aqueous solution, micelle formation by amphiphilic molecules, and the stability of lipid bilayers and biological membranes. The basis for hydrophobic interaction is usually assumed to be the unusual way in which nonpolar molecules and groups are hydrated in water. This unusual hydration is often called "hydrophobic hydration".

Computer simulation studies have contributed greatly to our understanding of the hydrophobic interaction. Pangali et al.[1] calculated the potential of mean force, or equivalently the solute–solute correlation function, for a pair of nonpolar solutes in water using their force-bias Monte Carlo technique. Their results indicated the existence of two relatively stable configurations for the solute atoms, in agreement with the earlier semiempirical theory of Pratt and Chandler.[2] One of these configurations corresponds to two solutes in contact. The interesting feature of the results was the greater stability of the second configuration, in which two solute atoms are separated by a water molecule. The existence of two stable configurations was also implied by two other computer simulation studies,[3,4] which calculated the mean relative force between nonpolar solutes in water.

Further insights into the problem of hydrophobic interaction were provided by molecular dynamics studies in which the motion of solutes in water was calculated. Geiger et al.[5] studied a system consisting of 2 Lennard-Jones solute atoms and 214 water molecules. The solute atoms, which were initially in contact, drifted to permit a single water molecule between them, resulting in a formation of vertex-sharing solvent cages containing the solutes. Using a similar approach, Rapoport and Scheraga[6] calculated the motions in a system composed of 4 solute atoms and 339 water molecules. The simulation was run for 70 ps, which was considerably longer than the run time of 8 ps used by Geiger et al. This simulation, however, failed to reveal any tendency for the initially well-separated solutes to associate. As pointed out by Rapoport and Scheraga, however, there is a possibility that the duration of their simulation was insufficient to permit observation of the association of solutes.

† Natural Sciences and Engineering Research Council of Canada postdoctoral fellow.

(1) C. Pangali, M. Rao, and B. J. Berne, *J. Chem. Phys.*, **71**, 2975 (1979).
(2) L. R. Pratt and D. Chandler, *J. Chem. Phys.*, **67**, 3683 (1977).
(3) C. S. Pangali, M. Rao, and B. J. Berne in "Computer Modeling of Matter", P. Lykos, Ed., American Chemical Society, Washington, D.C., 1978.
(4) S. Swaminathan and D. L. Beveridge, *J. Am. Chem. Soc.*, **101**, 5832 (1979).
(5) A. Geiger, A. Rahman, and F. H. Stillinger, *J. Chem. Phys.*, **70**, 263 (1979).
(6) D. C. Rapoport and H. A. Scheraga, *J. Phys. Chem.*, **86**, 873 (1982).

0022-3654/86/2090-0795$01.50/0